MALDI-TOF Mass Spectroscopy

Matrix-assisted laser desorption ionization/time of flight (MALDI/TOF) mass spectra were obtained on Ultraflextreme (Bruker Daltonics, Germany) mass spectrometer using sinapinic acid as matrix (Bruker Daltonics) in KBSI (Ohchang, Republic of Korea).

Size Exclusion-HPLC

Radiochemical purities of radioimmunoconjugates were analyzed by size-exclusion HPLC using a MAbPac SEC-1 column (Thermo Scientific). The mobile phase consisted of 0.3 M NaCl in 50 mM sodium phosphate buffer pH 6.8 and was eluted at a flow rate of 0.5 mL/min. The retention times of radioimmunoconjugates were determined from UV absorbance (Younglin Instrument Co., LTD) and radioactivity (GABI RI detector, Raytest).

***In Vitro* Stability Assay**

In vitro stabilities of ^{64}Cu-/^{177}Lu-PCTA-cetuximab were evaluated up to 24 h and 7 days, respectively. Each radioimmunoconjugate was added to human serum and incubated at 37°C. Samples were analyzed by ITLC-sg analysis at different time point.

Immunoreactivity Test

The immunoreactivity of radiolabeled cetuximab in TE-8 cells was determined according to the Lindmo method (*1*). ^{64}Cu-/^{177}Lu-PCTA-cetuximab (100 ng) were incubated with increasing concentration (1.25, 2.5, 5, 12.5 and 25 × 10^6 cells/mL, n = 3) of TE-8 cells. Nonspecific binding was evaluated with excess unlabeled cetuximab. After 1 h incubation, the samples were washed twice in cold PBS containing 1% BSA. Each sample was counted in a gamma counter (WIZARD 1480). The data were plotted as a double inverse plot of the applied radiolabeled antibody over the specific binding, as a function of the inverse cell concentration. Immunoreactivity index was calculated as the inverse intercept value at the ordinate.

Digital Whole-Body Autoradiography

After micro-SPECT/CT imaging, sacrificed mice were frozen at -70°C deep freezer. Mice were embedded in a mold on a microtome stage by adding an ice-cold aqueous solution of 3% carboxymethyl cellulose sodium salt (Wako Pure Chemical Industries). Coronal whole-body mouse sections (30 μm thick) were obtained by whole-

body autocryotome (Nakagawa Seisakusho). The frozen sections were exposed to an image plate for 24 h, and the plates were scanned with BAS-5000 image reader (Fujifilm).

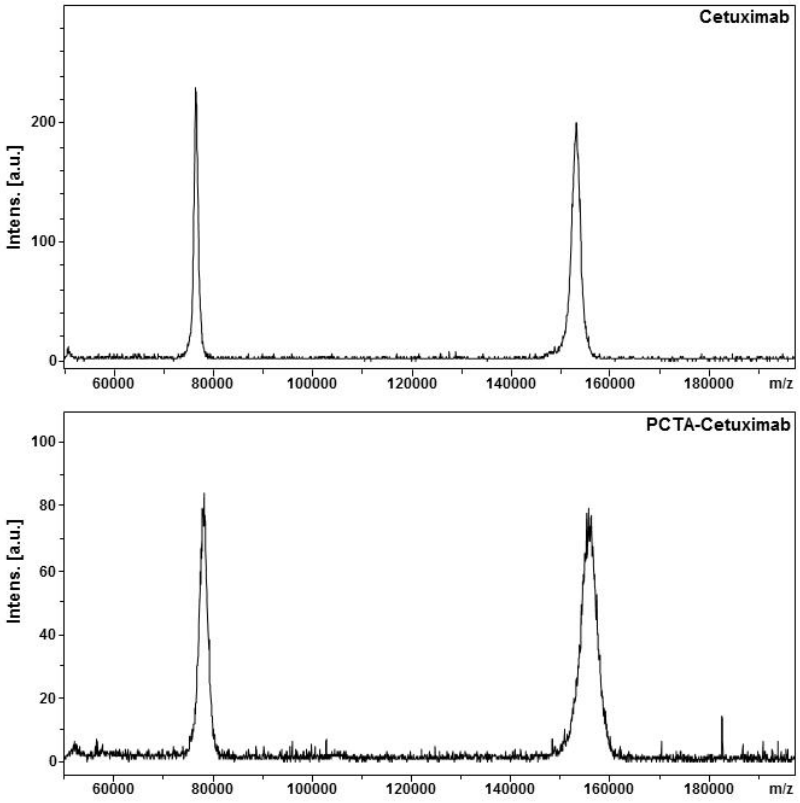

Supplemental Figure 1. MALDI-TOF mass spectra of cetuximab and PCTA-cetuximab. The difference in mass between the molecular peaks gives a degree of conjugation of 4.0 ± 0.4 macrocycles per antibody. a.u., arbitrary unit.

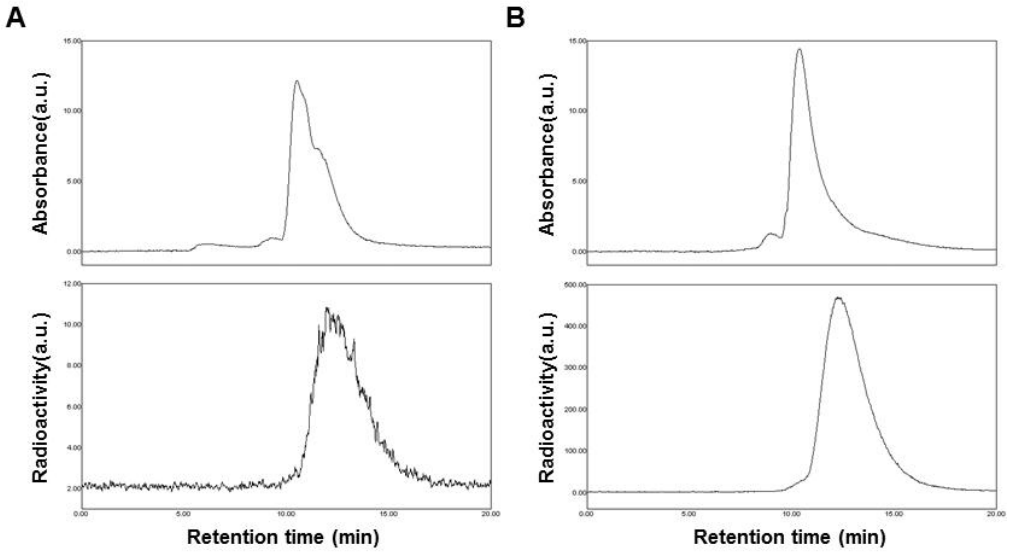

Supplemental Figure 2. Size exclusion-HPLC chromatograms of ^{64}Cu-PCTA-cetuximab (A) and ^{177}Lu-PCTA-cetuximab (B). Upper panels show the absorbance of the radioimmunoconjugates at 280 nm and lower panels show the radioactivity. a.u., arbitrary unit.

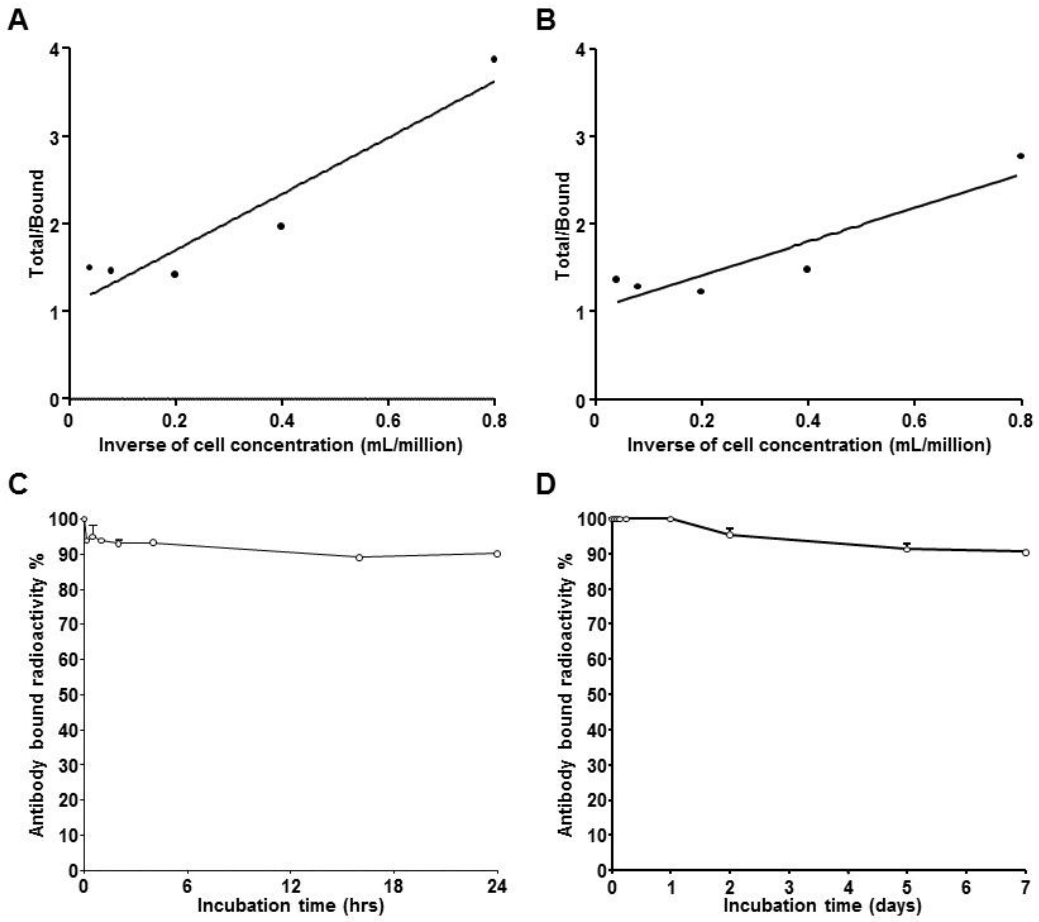

Supplemental Figure 3. Characteristics of ^{64}Cu-/^{177}Lu-PCTA-cetuximab. Immunoreactivities of ^{64}Cu-PCTA-cetuximab (A) and ^{177}Lu-PCTA-cetuximab (B). Iummunoreactive indices were 0.972 and 0.974, respectively. Serum stabilities of ^{64}Cu-PCTA-cetuximab (C) and ^{177}Lu-PCTA-cetuximab (D). The mixtures of serum and radioimmunoconjugates were incubated at 37°C. Both ^{64}Cu- and ^{177}Lu-cetuximab showed high stabilities (> 90%).

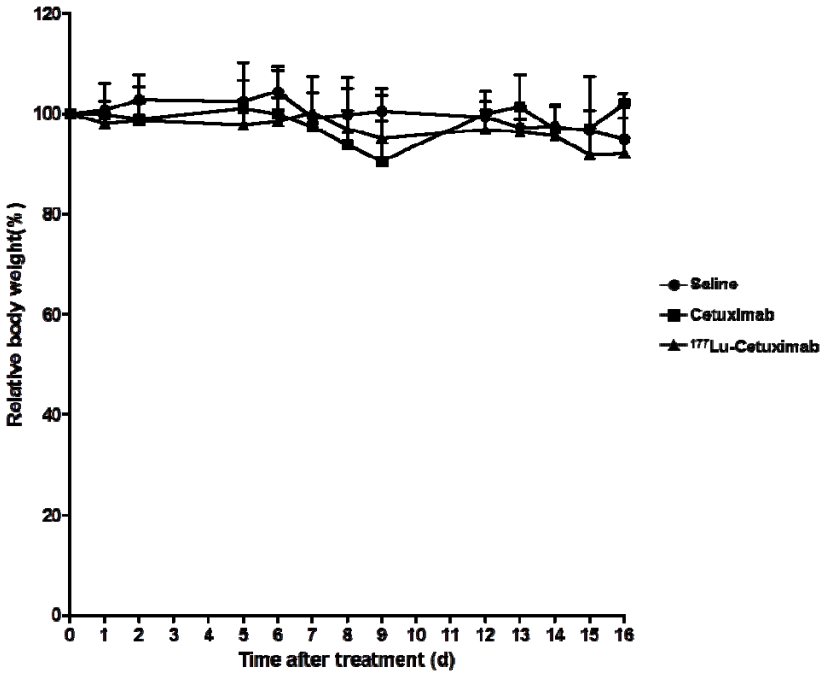

Supplemental Figure 4. Relative bodyweight changes over time in TE-8 tumor-bearing mice administrated with saline, cetuximab (5 mg/kg) and 12.95 MBq of ^{177}Lu-PCTA-cetuximab. No apparent body weight loss was observed in all groups.

Supplemental Table 1. Biodistribution of ^{64}Cu-PCTA-cetuximab in human ESCC tumor model.

	TE-4				TE-8			
	2 h	**24 h**	**48 h**	**72 h**	**2 h**	**24 h**	**48 h**	**72 h**
Blood	27.8 ± 3.5	9.0 ± 1.3	5.6 ± 0.7	3.7 ± 0.6	20.5 ± 1.9	6.4 ± 0.7	4.4 ± 0.8	2.5 ± 0.4
Heart	5.4 ± 0.6	3.0 ± 0.3	2.6 ± 0.2	2.1 ± 0.2	4.3 ± 0.7	3.0 ± 0.2	2.5 ± 0.1	1.9 ± 0.1
Liver	21.9 ± 0.7	12.5 ± 0.6	8.3 ± 0.4	5.6 ± 0.0	24.3 ± 2.0	13.1 ± 1.9	10.0 ± 1.3	7.2 ± 0.4
Lung	8.9 ± 0.1	4.7 ± 0.6	4.0 ± 0.2	3.2 ± 0.3	8.2 ± 0.5	5.0 ± 1.2	3.3 ± 0.5	2.7 ± 0.1
Spleen	12.4 ± 2.1	9.4 ± 1.5	7.1 ± 0.9	3.8 ± 0.6	9.9 ± 1.3	5.4 ± 1.3	3.9 ± 0.9	3.6 ± 1.2
Kidney	9.8 ± 1.0	5.0 ± 0.7	4.1 ± 0.1	3.3 ± 0.1	7.8 ± 0.7	4.2 ± 0.5	3.5 ± 0.3	2.6 ± 0.1
Stomach	1.4 ± 0.3	2.2 ± 0.3	1.7 ± 0.3	1.2 ± 0.2	2.2 ± 0.7	1.0 ± 0.2	1.3 ± 0.3	0.4 ± 0.1
Small Intestine	4.2 ± 0.3	3.1 ± 0.5	2.4 ± 0.2	1.7 ± 0.2	3.2 ± 0.4	2.2 ± 0.2	2.0 ± 0.3	1.3 ± 0.0
Large Intestine	1.3 ± 0.3	4.8 ± 0.7	3.2 ± 0.3	2.1 ± 0.2	3.1 ± 0.8	5.2 ± 2.5	2.7 ± 0.1	1.6 ± 0.2
Muscle	0.9 ± 0.1	1.5 ± 0.2	1.2 ± 0.1	0.9 ± 0.1	0.8 ± 0.1	1.3 ± 0.1	1.0 ± 0.2	0.7 ± 0.1
Femur	2.9 ± 0.1	1.8 ± 0.2	1.6 ± 0.1	1.1 ± 0.3	2.0 ± 0.3	1.7 ± 0.2	1.1 ± 0.2	0.8 ± 0.2
Tumor	2.7 ± 0.3	8.2 ± 0.7	9.0 ± 0.4	7.1 ± 1.0	5.7 ± 0.2	13.9 ± 0.5	17.5 ± 4.4	9.1 ± 1.0
T/B*	0.1 ± 0.0	0.9 ± 0.1	1.6 ± 0.1	1.9 ± 0.0	0.3 ± 0.0	2.2 ± 0.2	3.9 ± 0.6	3.7 ± 1.1
T/M**	2.9 ± 0.1	5.4 ± 0.7	7.4 ± 0.4	7.7 ± 1.4	7.1 ± 1.3	10.3 ± 0.4	17.0 ± 1.5	14.4 ± 3.7
T/L***	0.1 ± 0.0	0.7 ± 0.1	1.1 ± 0.1	1.3 ± 0.2	0.2 ± 0.0	1.1 ± 0.2	1.8 ± 0.7	1.3 ± 0.1

Data represent mean ± standard deviation (n = 3 or 4).

*, Tumor-to-blood ratio; **, Tumor-to-muscle ratio; ***, Tumor-to-liver ratio.

Supplemental Table 2. Biodistribution of ^{177}Lu-PCTA-cetuximab in TE-8 tumor models.

	2 h	1 d	3 d	5 d	5 d (blocking)	7 d	14 d
Blood	30.2 ± 1.0	12.1 ± 1.0	6.0 ± 3.5	3.1 ± 0.8	2.5 ± 0.5	1.1 ± 1.4	0.9 ± 0.6
Heart	6.1 ± 0.5	3.7 ± 0.3	1.8 ± 0.8	1.1 ± 0.2	1.3 ± 0.1	0.7 ± 0.3	0.6 ± 0.1
Liver	17.8 ± 0.3	14.9 ± 4.7	9.1 ± 0.9	5.3 ± 0.7	6.9 ± 0.2	5.5 ± 1.3	3.5 ± 0.5
Lung	9.8 ± 0.5	5.9 ± 1.2	3.4 ± 1.5	2.4 ± 0.3	2.1 ± 0.3	1.1 ± 0.8	1.2 ± 0.2
Spleen	10.3 ± 1.4	10.3 ± 4.0	8.1 ± 2.9	23.0 ± 6.1	5.7 ± 0.6	9.3 ± 6.5	5.3 ± 0.7
Kidney	10.9 ± 0.1	5.9 ± 0.5	3.2 ± 1.0	2.0 ± 0.2	1.6 ± 0.3	1.2 ± 0.6	1.1 ± 0.1
Stomach	1.4 ± 0.2	1.6 ± 0.3	1.0 ± 0.3	0.6 ± 0.2	0.6 ± 0.2	0.4 ± 0.1	0.3 ± 0.1
Small intestine	3.4 ± 0.1	2.0 ± 0.1	1.1 ± 0.3	0.7 ± 0.1	0.6 ± 0.1	0.3 ± 0.2	0.3 ± 0.1
Large intestine	2.1 ± 0.1	2.4 ± 0.4	1.8 ± 0.2	1.1 ± 0.3	0.6 ± 0.1	0.6 ± 0.3	0.3 ± 0.0
Muscle	1.3 ± 0.3	2.3 ± 0.3	0.9 ± 0.4	0.7 ± 0.1	0.7 ± 0.1	0.3 ± 0.2	0.3 ± 0.1
Femur	2.1 ± 0.3	2.7 ± 0.1	2.2 ± 0.6	1.9 ± 0.1	1.5 ± 0.2	1.6 ± 0.3	2.1 ± 0.2
TE-8	7.1 ± 1.0	38.3 ± 14.5	44.5 ± 15.2	55.7 ± 6.5	11.6 ± 0.4	37.8 ± 20.3	26.1 ± 10.9
T/B*	0.2 ± 0.0	3.3 ± 1.5	8.5 ± 2.9	18.9 ± 6.0	4.8 ± 0.9	59.5 ± 37.8	32.1 ± 8.7
T/M**	5.8 ± 1.2	16.0 ± 4.2	49.9 ± 9.1	77.5 ± 8.4	17.5 ± 2.6	128.1 ± 26.8	77.6 ± 22.4
T/L***	0.4 ± 0.1	2.8 ± 1.3	4.9 ± 1.5	10.7 ± 2.4	1.7 ± 0.1	7.1 ± 3.6	7.6 ± 3.8

Data represent mean ± standard deviation (n = 4).

*, Tumor-to-blood ratio; **, Tumor-to-muscle ratio; ***, Tumor-to-liver ratio.

REFERENCES

1. Lindmo T, Boven E, Cuttitta F, Fedorko J, Bunn PA Jr. Determination of the immunoreactive fraction of radiolabeled monoclonal antibodies by linear extrapolation to binding at infinite antigen excess. *J Immunol Methods*. 1984;72:77-89.